

RESEARCH ARTICLE

10.1002/2017MS001129

Key Points:

- Improvement of seasonal forecast of summer monsoon rainfall due to better ocean initial state to coupled forecast system
- Assimilation of ARGO actual salinity profiles to the global data assimilation system leads to realistic ocean state
- Better upper ocean heat content supports air-sea interaction and provides reasonable moisture to the atmosphere crucial to seasonal forecast

Correspondence to:

A. Parekh,
anant@tropmet.res.in

Citation:

Koul, V., Parekh, A., Srinivas, G., Kakatkar, R., Chowdary, J. S., & Gnanaseelan, C. (2018). Role of ocean initial conditions to diminish dry bias in the seasonal prediction of Indian summer monsoon rainfall: A case study using climate forecast system. *Journal of Advances in Modeling Earth Systems*, 10, 603–616. <https://doi.org/10.1002/2017MS001129>

Received 24 JUL 2017

Accepted 6 FEB 2018

Accepted article online 9 FEB 2018

Published online 2 MAR 2018

© 2018. The Authors.

This is an open access article under the terms of the Creative Commons Attribution-NonCommercial-NoDerivs License, which permits use and distribution in any medium, provided the original work is properly cited, the use is non-commercial and no modifications or adaptations are made.

Role of Ocean Initial Conditions to Diminish Dry Bias in the Seasonal Prediction of Indian Summer Monsoon Rainfall: A Case Study Using Climate Forecast System

Vimal Koul^{1,2,3,4}, Anant Parekh¹ , G. Srinivas¹, Rashmi Kakatkar^{1,2} , Jasti S. Chowdary¹ , and C. Gnanaseelan¹ 

¹Climate Variability and Data Assimilation Research, Indian Institute of Tropical Meteorology, Pune, India, ²Department of Atmospheric and Space Sciences, Savitribai Phule Pune University, Pune, India, ³Climate Modelling, Institute of Oceanography, Universität Hamburg, Hamburg, Germany, ⁴International Max Planck Research School on Earth System Modelling, Max Planck Institute for Meteorology, Hamburg, Germany

Abstract Coupled models tend to underestimate Indian summer monsoon (ISM) rainfall over most of the Indian subcontinent. Present study demonstrates that a part of dry bias is arising from the discrepancies in Oceanic Initial Conditions (OICs). Two hindcast experiments are carried out using Climate Forecast System (CFSv2) for summer monsoons of 2012–2014 in which two different OICs are utilized. With respect to first experiment (CTRL), second experiment (AcSAL) differs by two aspects: usage of high-resolution atmospheric forcing and assimilation of only ARGO observed temperature and salinity profiles for OICs. Assessment of OICs indicates that the quality of OICs is enhanced due to assimilation of actual salinity profiles. Analysis reveals that AcSAL experiment showed 10% reduction in the dry bias over the Indian land region during the ISM compared to CTRL. This improvement is consistently apparent in each month and is highest for June. The better representation of upper ocean thermal structure of tropical oceans at initial stage supports realistic upper ocean stability and mixing. Which in fact reduced the dominant cold bias over the ocean, feedback to air-sea interactions and land sea thermal contrast resulting better representation of monsoon circulation and moisture transport. This reduced bias of tropospheric moisture and temperature over the Indian land mass and also produced better tropospheric temperature gradient over land as well as ocean. These feedback processes reduced the dry bias in the ISM rainfall. Study concludes that initializing the coupled models with realistic OICs can reduce the underestimation of ISM rainfall prediction.

Plain Language Summary Seasonal forecast of summer monsoon is sensitive to the upper ocean state mainly over the tropical ocean. This upper ocean state is constituted by the temperature and salinity structure, errors in these fields can mislead the seasonal forecast. Present study demonstrated that apart from actual temperature profile data, salinity profile observations based ocean reanalysis produced better ocean state. This revised ocean reanalysis based ocean initial conditions are used for the hindcast of 2012 to 2014 summer monsoon and found improvement in the seasonal forecast. Prominent dry bias in seasonal forecast of rainfall over the monsoon core region as well as over the all India is getting reduced more than 10%, which is even higher than the variability of the summer monsoon. Detail analysis brought out that improvement in the upper ocean heat content forecast supported realistic air sea interaction in the coupled model and provided reasonable moisture to the atmosphere. This leads to better forecast of moisture transport associated with the summer monsoon resulting reduction in the precipitation biases over the India as well as neighboring oceanic regions. Overall the present study confirms that realistic ocean state in the initial condition is vital for accurate seasonal forecast of Indian summer monsoon.

1. Introduction

The dynamical seasonal prediction of Indian summer monsoon (ISM) is currently being pursued actively using coupled models (Kim et al., 2012; Kumar et al., 2005; Pokhrel et al., 2016; Zhu & Shukla, 2013). The seasonal predictions mostly rely on the slowly evolving boundary conditions such as sea surface temperature (SST), soil moisture, Eurasian snow cover etc. (Charney & Shukla, 1981; Palmer & Anderson, 1994). In addition

to that seasonal variability of ISM rainfall is largely controlled by the coupled ocean-atmosphere processes such as El Niño Southern Oscillations (ENSO; Kumar et al., 1995; Pant & Parthasarathy, 1981; Rasmusson & Carpenter, 1983; Sikka, 1980; Webster & Yang, 1992) and Indian Ocean Dipole (IOD, Ashok et al., 2001). Therefore, India adopted National Centers for Environmental Prediction (NCEP) coupled dynamical prediction system, Climate Forecast System version 2 (CFSv2) for the seasonal forecast of ISM rainfall (http://www.tropmet.res.in/monsoon/files/about_us.php). This coupled general circulation system includes atmosphere, ocean, and land surface models. It displayed improvement in the seasonal forecast of air temperature and SST but no improvement is reported for the precipitation over the land (e.g., Saha et al., 2014) with respect to previous version. As far as the seasonal prediction of ISM rainfall is concerned CFSv2 displays dry rainfall bias over the Indian land mass. Which could possibly be due to cold troposphere, low cloud fraction, and underestimation of high clouds and cold SST (De et al., 2016; Hazra et al., 2015). Further they suggested the need of modification of microphysical processes in the warm phase and mixed phase clouds for realistic representation of cloud and precipitation in CFSv2. Apart from this, Goswami et al. (2014) reported that synoptic variance is lower than the intraseasonal variance in CFSv2 especially over the Indian land mass leading to the underestimation of ISM rainfall. They attributed this to the deficiency in the convective parameterization in CFSv2. Subsequently, Ganai et al. (2015) reported that misrepresentation of diurnal cycle significantly contributes to the dry bias and suggested that cloud parameterization with realistic deep convection could improve diurnal rainfall, which in turn improves ISM rainfall. Bombardi et al. (2016) on the other hand suggested that inclusion of deep convection in the heated condensation frame work as an additional criterion in the simplified Arakawa-Schubert scheme improved the background state of convection and realistic frequency of deep convection. This leads to the better representation of ISM rainfall over the central and north eastern India. In addition to that the net surface radiation also improved, which is otherwise underestimated in CFSv2 compared to NASA/GEWEX (Goswami et al., 2017). Narapusetty et al. (2015) found that CFSv2 based seasonal forecast of northward migration of ITCZ is not accurate leading to the dry bias in the summer over the India. Chowdary et al. (2015) and Pokhrel et al. (2012) have reported that the excess evaporation in the model misrepresents the ocean-atmosphere interaction apart from radiative fluxes. These above discussed biases strongly suggest the possibility of further improvement in the adopted CFSv2 for better seasonal prediction of ISM rainfall.

Several studies in the past have explored the impact of accurate surface and subsurface ocean states on the dynamical seasonal predictions of El Niño and the Southern Oscillation (ENSO; Alves et al., 2004; Fischer et al., 1997; Ji & Leetmaa, 1997, etc.). They argued that the impact of subsurface ocean data assimilation has the potential to mitigate to some extent the impact of errors in wind-stress forcing and model errors, resulting in an improved seasonal prediction in a coupled ocean atmosphere forecasting system. Yang et al. (2010) reported improvement in the prediction of 2006 El Niño features and the spatial extent of the warm pool, while using salinity observations for the preparation of OICs. Further study by Zhao et al. (2013) found that initialization of subsurface near and off equatorial salinity may be as important as the initialization of ocean temperatures, for long range prediction. Zhao et al. (2014) also showed that better initial salinity field in the western Pacific could improve prediction of the Nino3.4 SST index as well as subsurface temperatures in the Indian Ocean. Improvements are brought about by fresh anomalies at the equator which increases stability, reduces mixing, and shoals the thermocline which concentrates the wind impact of ENSO coupling. This effect is most pronounced in June–August, helping to explain the improvement. Huang et al. (2008) showed that inclusion of actual Argo salinity profiles in National Centers for Environmental Prediction (NCEP) Global Ocean Data Assimilation System (GODAS) reduced biases (errors) of zonal current in the tropical Indian Ocean by 5–10 (2–5) cm s^{-1} . Deshpande et al. (2017) reported that variability of zonal current in the equatorial Indian Ocean, alters ISM by modulating the monsoon Hadley circulation. Balmaseda and Anderson (2009) also reported that Argo has a larger effect in the Indian Ocean. Kakatkar et al. (2017) highlights the importance of maintaining observing systems such as ARGO for accurate monsoon forecast. Fousiya et al. (2015) also showed that assimilation of actual salinity profiles in GODAS brings the Bay of Bengal (BoB) to a more realistic state and captures BoB barrier layer variability (e.g., Agarwal et al., 2012; Thompson et al., 2006). Formation of barrier layer in fact influences the air-sea interaction ranging from synoptic to intraseasonal scale systems over the region which are contributing significantly to the ISM rainfall (Goswami et al., 2003; Mooley & Shukla 1989). Hence, it is mandatory that the OICs for the coupled models be as realistic as possible for a skillful seasonal prediction of ISM.

Historically, lack of salinity observations, particularly subsurface, has eluded proper representation of salinity in ocean analyses. Recently operational centers around the world have improved salinity representation in

their respective ocean analyses. One way to do that is by using synthetic salinity profiles generated for each temperature profile using local T-S climatology. This is better than using climatological salinity which underestimates salinity variability in some basins. The other way to get accurate realistic upper ocean state for seasonal prediction of ISM is to assimilate surface and subsurface observations of ocean temperature and salinity from Argo (Array of real time geostrophic oceanography, Argo Science Team, 2001) with appropriate assessment while keeping in mind that methodology adopted for data assimilation impacts the accuracy of OICs (Kalnay, 2002). Above discussions motivated us to carry out the present study where two different initial state of ocean are used as OICs in CFSv2, first initial state is based on the traditional ocean reanalysis NCEP-GODAS and the second initial state is produced using high-resolution forcing and assimilating actual salinity and temperature profiles from Argo i.e., Indian Institute of Tropical Meteorology GODAS (IITM-GODAS). Thus, the coupled model experiments are initialized with differing OICs to study the impact of OICs on hindcast of summer monsoon features, an unexplored area in the ISM forecasting system. Section 2 provides details about the data used, model and the experiments carried out in this study. In section 3, results from experiments are discussed and section 4 derives main conclusion.

2. Data and Methodology

Gridded rainfall data sets from the India Meteorological Department (IMD, Pai et al., 2014) and Global Precipitation Climatology Project v2.2, (GPCP, Adler et al., 2003) are used to evaluate model rainfall during summer of 2012–2014. European Centre for Medium-Range Weather Forecasts (ECMWF) Reanalysis Interim (ERA, Dee et al., 2011) fields of winds, moisture, and air temperature are used for comparing corresponding model fields. Objectively analyzed air-sea fluxes (OAflux, Yu & Weller, 2007) are used for evaluating evaporation rate. Hadley centre observations data set (EN4.1.1, Good et al., 2013) and Hadley centre Sea Ice and Sea Surface Temperature data set (HadISST, Rayner et al., 2003) are used for evaluating sea water temperature. Hybrid coordinate ocean model (HYCOM, Cummings, 2005; Cummings & Smedstad, 2013) daily analysis (GLBu0.08/expt_91.1) is used to compare OICs. The system used for generating HYCOM analysis is the Navy Coupled Ocean Data Assimilation. The assimilation scheme is 3DVar. It assimilates observations of SST, sea-ice concentration, and sea surface height from satellites and in situ observations of temperature, salinity, and ocean currents from ships, buoys, XBTs, and Argo. All of these data sets have been regridded wherever necessary to a common lower resolution of $1^\circ \times 1^\circ$. The monsoon core region (MCR, 18°N – 28°N 65°E – 88°E), which is a region representative of both the variability and strength of ISM rainfall (Rajeevan et al., 2010) the region covering all land points of India, which quantifies the total rainfall received during ISM (Parthasarathy et al., 1995) are selected for detailed analysis. According to IMD, in 2012, ISM rainfall was 93% of long period average, however for 2013 it was 106% and for 2014 it was 88%. In 2012, June and July received very scanty rain (72% and 87%, respectively) and August and September received better rainfall (101% and 112%, respectively). In case of 2013, above normal rainfall received in June and July and below normal in August and September. In case of 2014, all the 4 months received below normal rainfall with June receiving deficient rain, resulting 2014 summer monsoon deficient. Overall all the above 3 years cover the extremes of the ISM rainfall with wide spread in their evolution.

2.1. Model and Experiment Details

The NCEP CFSv2 (Saha et al., 2014, details therein) is a fully coupled atmosphere-ocean-land-surface-sea-ice dynamical model developed by NCEP. The atmospheric model in CFSv2, is Global Forecast System, which is configured at T126 horizontal resolution. The ocean model is Geophysical Fluid Dynamics Laboratory (GFDL) Modular Ocean Model (MOM) version 4p0d (Griffies et al., 2004). For the first experiment (CTRL) atmospheric initial conditions as well as OICs for CFSv2 are from NCEP climate prediction system reanalysis (NCEP-CFSR, Saha et al., 2010), available publicly at National Operational Model Archive and Distribution System data server. The NCEP generates OICs using state-of-the-art NCEP-GODAS (Behringer, 2007; Behringer & Xue, 2004; details therein). The ocean model in NCEP-GODAS is MOM3. The model has a horizontal resolution of $1/4^\circ$ in the North-South direction within 10° of the equator and it gradually increases to $1/2^\circ$ pole ward of 30° . The NCEP-GODAS is forced by the momentum flux, heat flux, and fresh water flux from the NCEP atmospheric reanalysis 2 (NCEPR2, Behringer & Xue, 2004). The NCEP-GODAS assimilates temperature profiles and synthetic salinity profiles using 3DVAR scheme. NCEP-GODAS assimilates temperature profiles from expendable bathythermographs (XBTs), in situ moorings and from Argo. Synthetic salinity profiles

are derived for each temperature profiles using local T-S climatology based on the annual mean fields of temperature and salinity.

The forecast system is initialized in May month to produce 9 month-lead forecasts for 2012, 2013, and 2014. There are 10 atmospheric initial conditions (10 ensemble member forecasts) partitioned into two segments. The first set uses five atmospheric initial states of the 1st, 2nd, 3rd, 4th, and 5th of May and uses the same pentad ocean initial condition centered on the 3rd of the same month. The second set uses the five atmospheric initial states of the 6th, 7th, 8th, 9th, and 10th of May and the same pentad ocean initial condition centered on the 8th of May. For the analysis, we have utilized ensemble mean forecasts obtained by averaging the above 10 ensemble members (Srinivas et al., 2017). NCEP-GODAS OICs are used in the CTRL experiment. However, in the second experiment (hereafter, AcSAL), same methodology is followed to produce hindcast, and the only difference being IITM-GODAS OICs are used. The atmospheric initial conditions for both the coupled model experiments (CTRL and AcSAL) are identical.

The data assimilation system in IITM-GODAS (Sreenivas et al., 2015), assimilates only quality controlled Argo observed salinity and temperature profiles. This is done to exclude the influence of associated synthetic salinity profiles which may in some locations exceed Argo salinity profiles (Huang et al., 2008). Apart from this during the study period number of Argos in the global ocean was consistently more than 3,500. The ocean model used for IITM-GODAS is quasi-global configuration of MOM4. The model domain extends from 75°S to 65°N and has a resolution of 1° by 1° enhanced to 1/3° in the north-south direction within 10° of the equator. The model has 40 vertical levels with a 10 m resolution in the upper 200 m. The model includes an explicit free surface, the Gent-McWilliams isoneutral mixing scheme, and the KPP vertical mixing scheme. Here, the ocean model MOM4 is forced by National Centre for Medium Range Weather Forecasting (NCMRWF) atmospheric forcing with 0.25° × 0.25° resolution and updated every 6 h (Rajagopal et al., 2012) which is based on Unified Model Based Analysis System. However, the NCEP-GODAS ocean analysis is forced by NCEP-R2 T62 resolution daily averaged surface forcing (Kanamitsu et al., 2002). Hence in IITM-GODAS spatial and temporal resolution of forcing is higher than NCEP-GODAS. High-resolution forcing to the ocean models supports better representation of mesoscale eddies, tropical instability waves and spatial gradients of SST. In IITM-GODAS, the model is run in 5 day increments and then 5 day averages of temperature and salinity are used to estimate the error variances for the next 5 day increment with an assimilation window of 10 days. Thus, IITM-GODAS produced ocean reanalysis at every pentad for the period of 2012–2014. The annual mean values of the UNESCO River runoff (Vörösmarty et al., 1996) have been used for freshwater forcing. Rahaman et al. (2016) carried out extensive study with different sensitivity experiments with the GODAS system. They reported that the assimilation of actual salinity profiles and high-resolution atmospheric forcing from NCMRWF-based GODAS simulation could produce better vertical structure of temperature and salinity, and also captures the important features such as equatorial currents, seasonal, and interannual variability, IOD, sub surface temperature inversion, sea level evolution over the tropical Indian Ocean more realistically compared to the NCEP GODAS. In data assimilation systems based on GODAS, the system assimilates synthetic salinity profiles calculated from the available temperature profiles at that grid point. By excluding temperature profiles from all sources other than Argo, we prevent assimilation of synthetic salinity profiles and their impact on the quality of OICs.

3. Result and Discussion

3.1. Assessment of Ocean Initial Conditions

In this section NCEP-GODAS and IITM-GODAS produced OICs of 3 May and 8 May of 2012–2014 are assessed with respect to HYCOM global analysis (Cummings, 2005). Comparison of NCEP-GODAS with HYCOM upper ocean temperature (averaged up to 125 m) (Figure 1a, for 8 May 2014) shows that NCEP-GODAS has cold bias over the tropics, stronger cold bias is seen over the eastern Pacific, equatorial Indian Ocean, along the western coast of Africa, and equatorial Atlantic Ocean. IITM-GODAS initial conditions display large reduction in bias over the tropics except over the Atlantic Ocean (Figure 1b). Major reduction in biases is also seen in the eastern Pacific and around the equatorial Indian Ocean (Figure 1b). Temperature over these two oceanic areas is critical for the ISM performance (Ashok et al., 2001; Kumar et al., 1995). The intensity of cold bias in NCEP-GODAS is more evident in Figure 1c. Statistical analysis (Table 1) shows that root mean square error (RMSE) in the upper ocean temperature (averaged up to 125 m) in IITM-GODAS (NCEP-GODAS) is 2.78°C

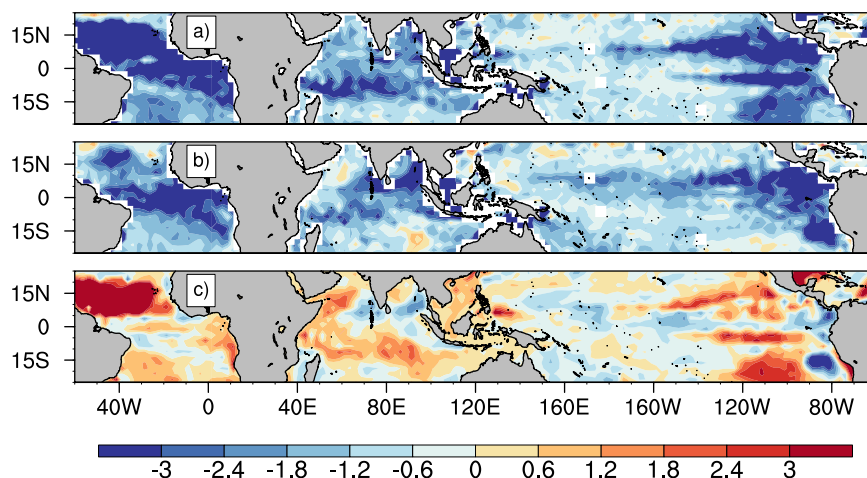


Figure 1. Spatial distribution of upper ocean (up to 125 m) temperature biases (°C) with respect to the HYCOM ocean analysis in ocean initial condition produced by (a) NCEP-GODAS, (b) IITM-GODAS, and (c) their differences for 8 May 2014.

(2.98°C) over the global tropics. Upper ocean displays reduced cold bias over the equatorial and western Indian Ocean between 10°S and 10°N in IITM-GODAS compared to NCEP-GODAS (Figure 1c) (difference of about 2–3°C for 2012 and 2013, figures not shown). Significant reduction in cold bias is also seen in the northern seas off maritime continent in IITM-GODAS. Thus, over the global tropics IITM-GODAS OICs have realistic heat content in the upper ocean with noticeable improvement compared to NCEP-GODAS OICs. This realistic heat content is a major differentiator as far as the present experiments are concerned. This supports the fact that actual salinity profile assimilation with high-resolution atmospheric forcing improves the upper ocean thermal state in the ocean reanalysis. Sreenivas et al. (2015) carried out detailed validation of IITM-GODAS with the independent buoy observations for the period of 2005–2014. They reported that actual salinity profile assimilation improved the interannual variability of ocean state over the BoB, extent of warm pool, salinity, mixed layer, isothermal, and thermocline depth. Rahaman et al. (2016) and Karmakar et al. (2017) also reported that actual salinity assimilation based ocean reanalysis represents accurate Indian Ocean state.

3.2. Assessment of Precipitation in Hindcast Experiments

This section describes the differences in the ISM features in the two coupled model experiments and discusses the associated processes. Monthly and seasonal mean rainfall over MCR and Indian land mass are shown in Figures 2a–2c and 2d–2f, respectively, from CTRL, AcSAL, GPCP, and IMD for the year 2012, 2013, and 2014. Both the experiments capture the seasonal evolution of rainfall over the Indian land mass as well as over the MCR. This analysis further reveals that both CTRL and AcSAL mostly underestimate the seasonal mean ISM rainfall, as well as monthly mean rainfall. It is important to note that the dry bias in AcSAL is less compared to CTRL. Further the reduction in bias in AcSAL is consistently apparent in each month as well as the season as a whole. Ramu et al. (2016) reported that cold bias in SST and tropospheric temperature leads to weaker meridional temperature gradient in CFSv2, resulting weaker low level monsoon circulation. Which negatively feeds back to tropical easterly jet and vertical wind shear. The under estimation of vertical wind shear of monsoon circulation leads to slow northward propagation of ISO in CFSv2 (Goswami et al., 2014). It is also found that due to weaker monsoon circulation moisture transport to the Indian land mass is underestimated resulting dry bias over Indian land mass in CTRL. The maximum negative bias of rainfall is seen during July and August (by greater than 2 mm d⁻¹); however, during June and September it is less than 2 mm d⁻¹. Quantitative analysis shows reduction of dry bias in AcSAL by 10% (Table 2), and the highest reduction in bias is reported for June.

On the other hand, 2014 season displays highest improvement (Table 2) consistent with the improvement in OICs (Figure 1).

Figure 3 displays the spatial distribution of rainfall biases for CTRL and AcSAL over the Indian land mass with respect to IMD observed rainfall and also the difference between the two experiments for the years

Table 1
Percentage Improvement in Precipitation Over MCR and All India (AI)

% Improvement	2012	2013	2014
MCR	5.8%	12.7%	19.1%
AI	9.6%	7.3%	15.4%

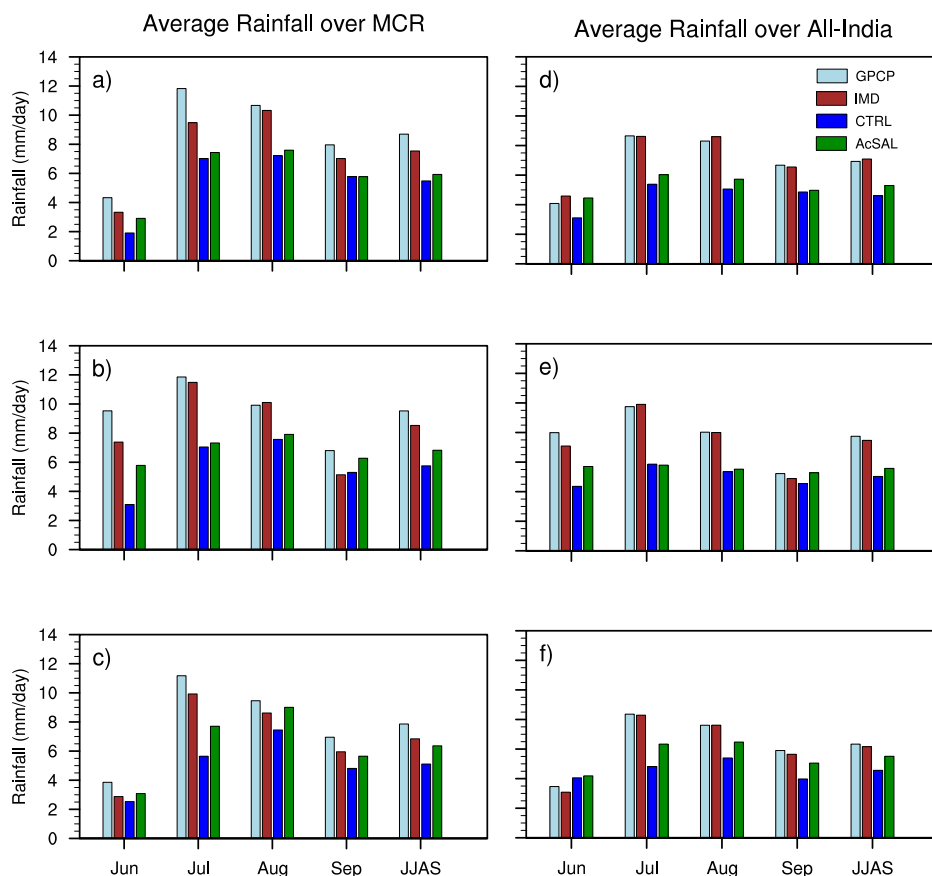


Figure 2. Monthly and seasonal mean precipitation (mm d^{-1}) over (a–c) MCR and (d–f) All-India for 2012, 2013, and 2014, respectively.

2012, 2013, and 2014. CTRL displays strong negative bias -4 to -6 mm d^{-1} over the central India, western India, some part of eastern India, and along the Western Ghats and displayed weaker positive bias ($1-2 \text{ mm d}^{-1}$) over the peninsular India, north India, and some part of eastern India (Figures 3a–3c). Among the 3 years 2013, an excess monsoon year (106%) displays strongest negative bias. In AcSAL, the spatial distribution of bias pattern is similar to CTRL but the strength of the negative bias over the central and western India is reduced by greater than 1 mm d^{-1} (Figures 3d–3f). Overall noticeable reduction ($\sim 2-3 \text{ mm d}^{-1}$) in negative bias of rainfall is seen over the MCR when IITM OICs are used (Figures 3g–3i). Table 3 further confirms that error in precipitation prediction is reduced over MCR as well as over AI in AcSAL. It is important to note that on an average the seasonal mean rainfall over the MCR is about $7-8 \text{ mm d}^{-1}$. Thus, the improvement in the land sea thermal contrast in AcSAL due to improvement in the OICs in the Indian Ocean by representing the realistic upper ocean stability and stratification. It is important to note that CTRL underestimates upper ocean stability over the Indian Ocean (Parekh et al., 2016). This realistic upper Ocean stability is leading to proper representation of upper ocean mixing favoring better upper ocean temperature forecast, which may be consequently supporting better air-sea interaction, monsoon circulation, and moisture transport compared to CTRL. This in turn improving the spatial and temporal pattern of rainfall over the Indian land mass. Which might have further feedback to tropospheric temperature, troposphere circulation, and the propagation of monsoon is positively feeding back to the reduction of rainfall biases over the northern and north western land mass of India.

Table 2
RMSE of Ocean Initial Conditions of SST (C) With Respect to HYCOM Ocean Analysis

Domain/ RMSE ($^{\circ}\text{C}$)	IITM-GODAS	NCEP-GODAS
IO ($25^{\circ}\text{S};25^{\circ}\text{N}, 40;110^{\circ}\text{E}$)	2.76	2.99
PO ($25^{\circ}\text{S};25^{\circ}\text{N}, 120;280^{\circ}\text{E}$)	2.49	2.63
Global	1.97	1.99
Global Tropics ($25^{\circ}\text{S};25^{\circ}\text{N}$)	2.78	2.99

3.3. Assessment of Moisture Fields in Hindcast Experiments

Above discussed improvements in the rainfall estimates in AcSAL with respect to CTRL led us to explore the associated variables. First, we

Table 3
 Root Mean Square Error (mm d^{-1}) in Precipitation Prediction of Two Experiments

RMSE (mm d^{-1})	2012		2013		2014	
	AcSAL	CTRL	AcSAL	CTRL	AcSAL	CTRL
MCR	3.7	4.1	4.3	4.8	2.7	3.3
AI	4.5	4.7	4.8	5.3	3.8	4.1

assess the atmospheric moisture content and its vertical distribution over the Indian land region and adjoining seas. This is an obvious choice since during monsoon moisture is advected from ocean toward land. Figures 4a–4c display vertical profile of specific humidity bias in the CTRL and AcSAL with respect to ERA specific humidity profiles and their differences over MCR during 2012, 2013, and 2014 ISM. In all the cases, both experiments display drier troposphere compared to ERA. However, in case of AcSAL the dry bias is less than that of CTRL for all the 3 years. In the lower troposphere the reduction in the dry bias is about 0.5–0.75 g kg^{-1} . This reduction in bias is maximum (minimum) during 2014 (2013). The improvement is almost constant up to mid troposphere and gradually decreasing above it. Similar analysis of moisture profile is carried out for the Arabian Sea (AS) and BoB. Figures 4d–4f display the vertical profile of specific humidity bias in the CTRL and AcSAL with respect to ERA and their differences for the AS during 2012, 2013, and 2014 ISM. Over AS the systematic bias in specific humidity is reduced throughout the column in AcSAL; more reduction in specific humidity bias is found from 925 to 600 hPa. So, it is clear that seasonal mean bias in specific humidity is reduced by about 20% in the lower troposphere due to more realistic ocean initial state and the improvement in the associated air-sea interaction in the model. However, improvement in the moisture distribution over the BoB is relatively meager. Earlier studies have shown that AS evaporation and

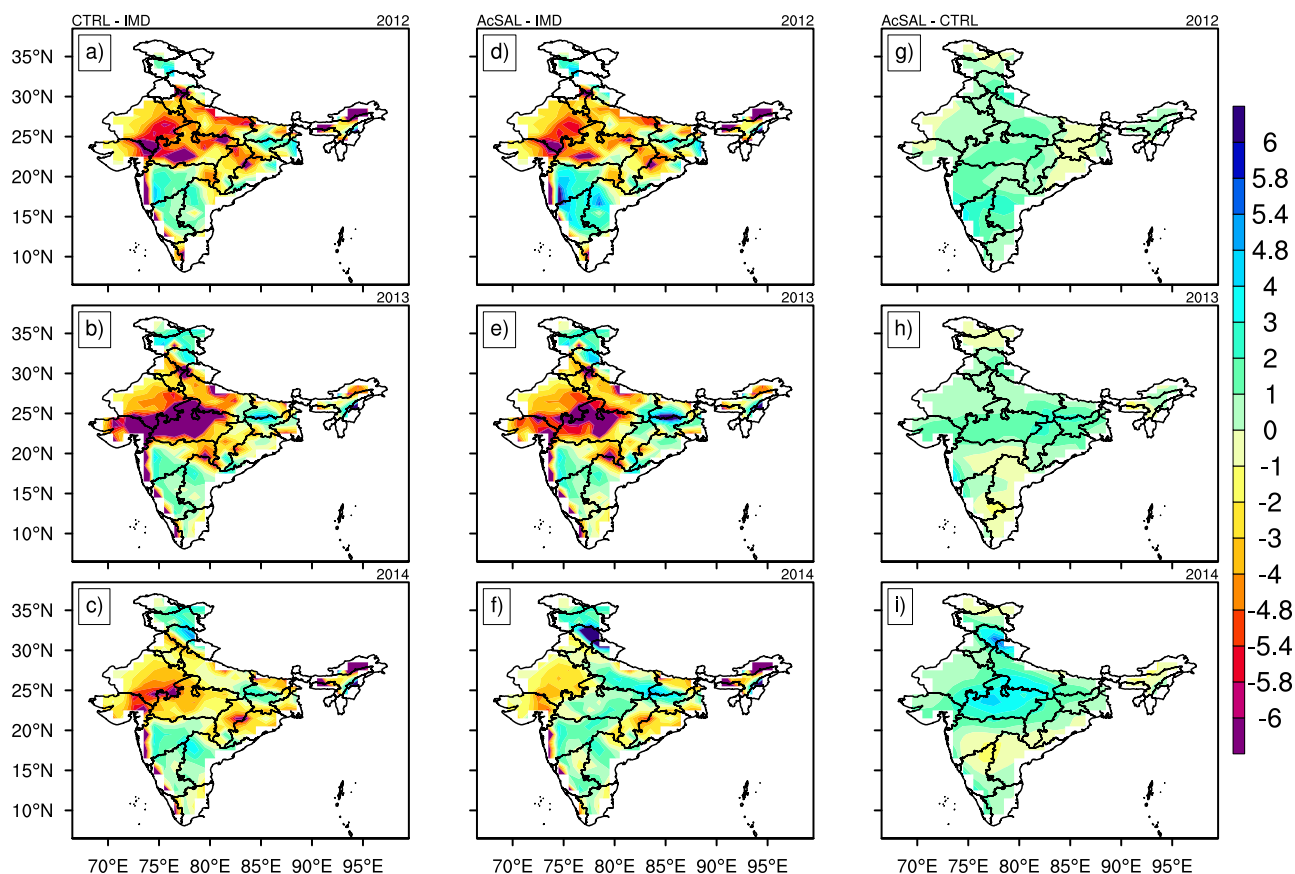


Figure 3. Spatial distribution of seasonal (JJAS) mean precipitation bias (mm d^{-1}) in (a–c) CTRL and (d–f) AcSAL with respect to IMD observations for 2012, 2013, and 2014. Also shown is the difference between the two experiments (g–i, AcSAL-CTRL).

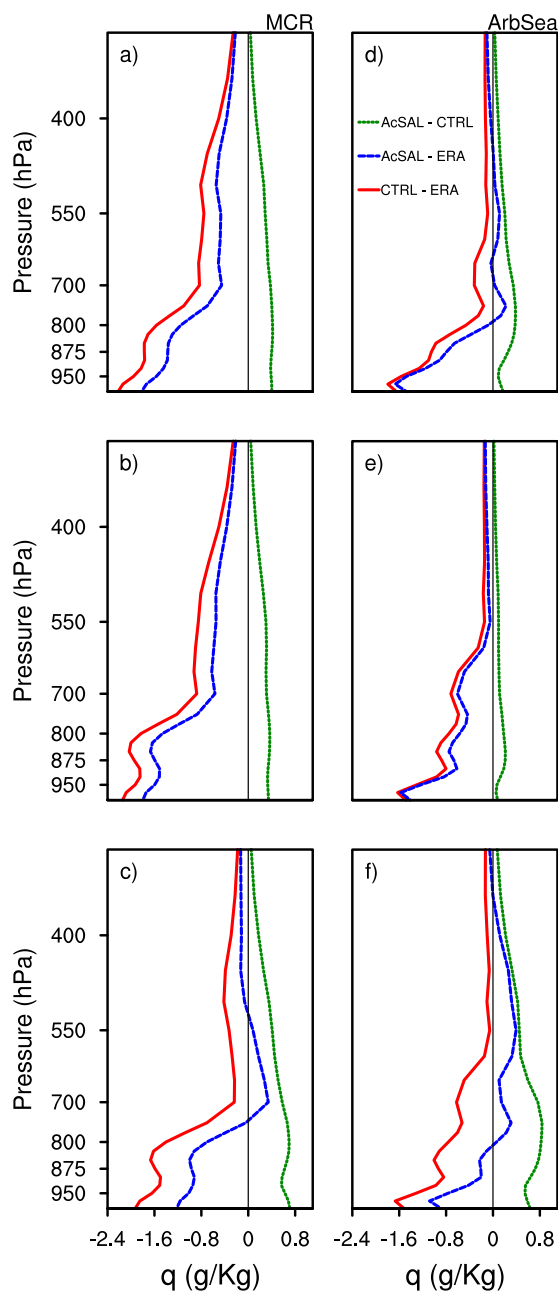


Figure 4. Seasonal (JJAS) mean bias in specific humidity (g kg^{-1}) over (a–c) MCR and over (d–f) Arabian Sea with respect to ERA for 2012, 2013, and 2014.

moisture transport from the south Indian Ocean are the main moisture sources of ISM rainfall (Levine & Turner, 2012; Pisharoty, 1965; Saha & Bavadekar, 1973). Recently, Pathak et al. (2017) also reported that during the monsoon more than 70% moisture to the Indian land mass is supplied mostly from the southern Indian Ocean, AS, and BoB. This moisture transport is mostly done by the lower tropospheric monsoon circulation which is south easterly (south westerly) south (north) of the equator. These winds are forced by the land sea thermal contrast, which is more realistic in AcSAL than CTRL due to reduction in cold SST bias in the southern Indian Ocean (Figure 1c). Further, the reduction in SST cold bias supported better air-sea exchange through evaporation and rectifies the moisture production in the surrounding ocean. This improvement in evaporation is higher in the AS than BoB, which could be due to lesser mean evaporation over the BoB compared to AS (Shenoi et al., 2002), and low evaporation bias over BoB than AS (e.g., Pokhrel et al., 2012). This is responsible for the meager improvement in the vertical distribution of moisture over the BoB (though meager) in AcSAL compared to AS.

Given the improvements in moisture profiles over the AS and MCR, it is now interesting to confirm the improvement in the moisture transport over the study region. Figure 5 shows vectors representing bias in integrated moisture transport ($\text{kg m}^{-1} \text{s}^{-1}$) and integrated moisture (kg m^{-2}). Large negative bias in CTRL is reported over the central India, over South Africa, western Pacific and western Indian Ocean (along the monsoon winds), and weak positive bias is reported over the rest of the study area (Figures 5a–5c). The moisture transport in CTRL displays south westward and westward bias over the AS, central India, and BoB. Over Africa westward bias in transport is dominating, however in the equatorial Indian Ocean and south of it, eastward transport bias is dominating in CTRL. These discrepancies in moisture transport reduces moisture supply to the Indian region and hence do not feed the atmosphere over the Indian region. The integrated moisture shows more realistic values in AcSAL (Figures 5d–5f) as compared to CTRL. In AcSAL (Figures 5d–5f) the spatial distribution of dry bias remains almost the same as in CTRL, however the magnitude of bias is reduced significantly mainly over the AS (Figures 5g–5i), south east Africa, India, and maritime continent. Overall AcSAL hindcast shows better moisture transport associated with the monsoon circulation. Figures 8g–8i display the seasonal as well as monthly biases of integrated moisture over the Indian Ocean. Seasonal mean bias is mostly negative and it is reduced by more than $0.2\text{--}0.5 \text{ kg m}^{-2}$ during the 2012 and 2013 ISM, however it is greater than 2.0 kg m^{-2} during the 2014 ISM. Month wise analysis supports that highest reduction in bias is during September in all the years.

These factors are the most likely cause of significant reduction in rainfall biases. The primary source of moisture is evaporation from the ocean surface, which is manifested by the latent heat flux. The magnitude of evaporation rate in the CTRL is overestimated with respect to OA flux data over the entire study domain (figure not shown). The evaporation rate displays an average bias of more than 3 mm d^{-1} over the AS and 1.5 mm d^{-1} over the BoB. However, evaporation bias is lesser in AcSAL and notable reduction is reported over the AS. This supports that surface moist processes are more realistic in AcSAL due to improved evaporation from the ocean surface.

3.4. Assessment of Low Level Circulation and Tropospheric Temperature in Hindcast Experiments

Reversal of low level circulation over the Indian Ocean is considered as a mark of onset of monsoon and its variation reflects the monsoon variability. In Figure 6, vector shows bias in low level wind (850 hPa) in CTRL

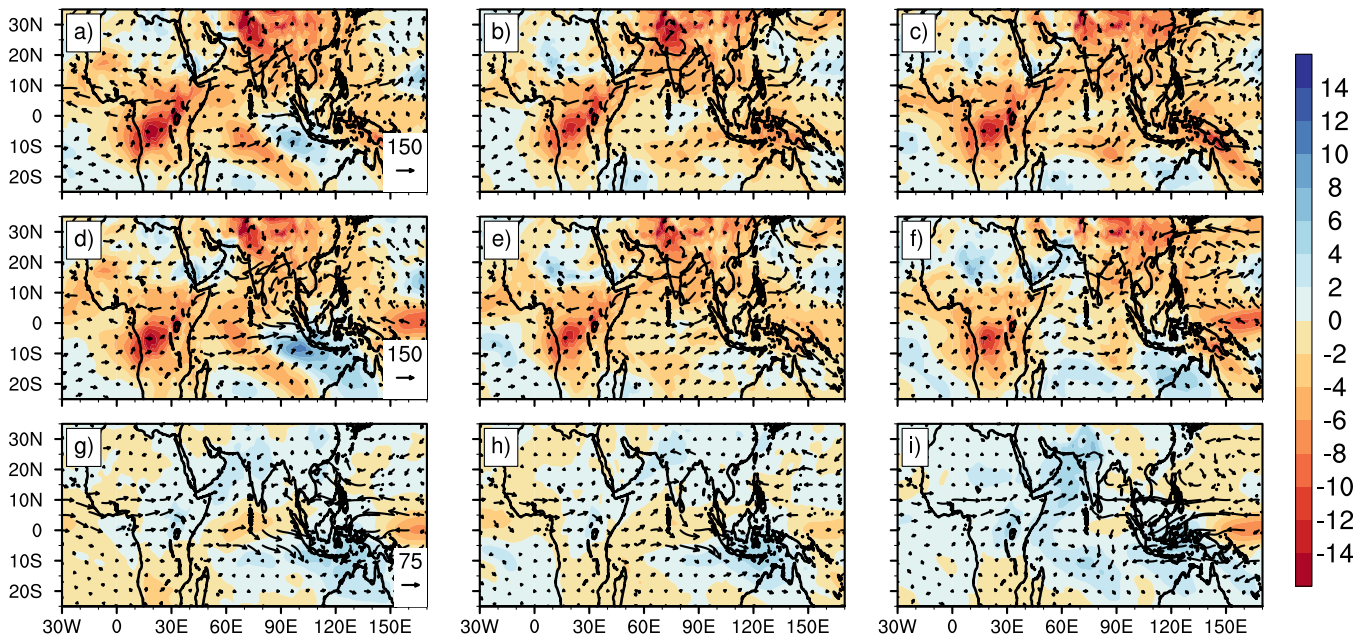


Figure 5. Spatial distribution of seasonal (JJAS) mean bias of vertically integrated moisture (shaded, kg m^{-2}) and vertically integrated moisture transport (vector, $\text{kg m}^{-1} \text{s}^{-1}$) in (a–c) CTRL, (d–f) AcSAL with respect to ERA, and (g–i) their difference (AcSAL–CTRL) for 2012, 2013, and 2014.

and AcSAL with respect ERA over the study region for years 2012, 2013, and 2014, respectively. This lower troposphere winds transport moisture to the Indian land mass. Figures 6a–6c clearly indicate that the strong westerly bias is reported south of 5°N in the Indian Ocean and over the India land mass northerly and north easterly biases are appeared, which is also true for the BoB. Narapusetty et al. (2015) also reported strong

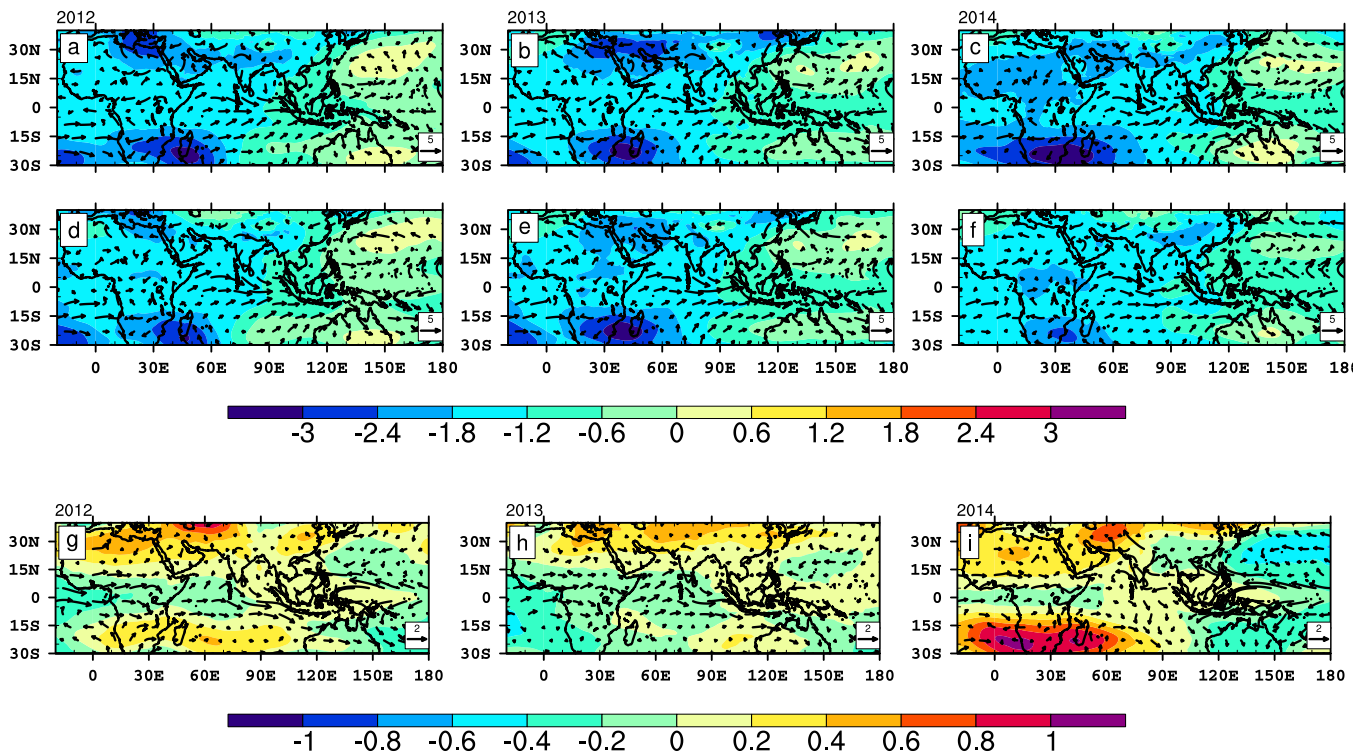


Figure 6. Spatial distribution of seasonal (JJAS) mean bias of Troposphere Temperature (shaded, $^{\circ}\text{C}$) and 850 hPa wind biases (vector, m s^{-1}) in (a–c) CTRL, (d–f) AcSAL with respect to ERA, and (g–i) their difference (AcSAL–CTRL) for 2012, 2013, and 2014.

westerly bias in the western central equatorial IO during the summer in CTRL. However, biases over the AS, BoB, and Indian land mass are reduced but the westerly bias south of the equator is increased in the AcSAL (Figures 6d–6f), which is more clear in the difference (Figure 6g–6i). Hence overall low-level winds display improvement over the Indian land mass and over the AS and BoB. Another important improvement is in the tropospheric temperature (TT), which is underestimated in the CTRL (Figures 6a–6c, shaded), here TT is estimated following Goswami and Xavier (2005, averaged between 700 and 200 hPa). Figures 6d–6f clearly show that TT underestimation is reduced in the AcSAL, over the land region (the north-north west part of study area) reduction in bias is higher than over the oceanic regions (Figures 6d–6f). This improvement clearly supports (Figures 6g–6i) that not only TT representation is getting improved in the AcSAL but representation of TT meridional gradient (difference of TT between a northern box [40–100°E, 5–35°N] and a southern box [40–100°E, 15°S–5°N]) is also getting improved by about 0.4°C. Ramu et al. (2016) reported that CFSv2 underestimates the meridional gradient by the 0.7°C and cold bias is much stronger over northern latitudes compared to southern latitudes. According to Goswami and Xavier (2005) and Xavier et al. (2007), the strength of this meridional gradient determines the intensity of monsoon. Hence reduction in TT bias and improvement in its meridional gradient positively feed back to the realistic representation of ISM in the AcSAL, which is consistent with the reduction of dry bias over the Indian land mass in AcSAL.

3.5. Assessment of SST and Heat Content in Hindcast Experiments

Further to understand reduction in biases, we studied SST biases in these two experiments. Figure 7 displays the seasonal bias in SST from CTRL (Figures 7a–7c), AcSAL (Figures 7d–7f), and their differences (AcSAL-CTRL, Figures 7g–7i). CTRL has colder SST in most of the Indian Ocean, north BoB, and along the Indonesia coast. In case of AcSAL, the cold biases over the Indian Ocean is reduced mainly over south of equator, western AS and BoB. It is important to note that the reduction in the cold bias of forecasted SST is highest in 2014 than the rest of the 2 years (Figure 7g–7i). Above mentioned improvement support more realistic air-sea interaction and supply of moisture through evaporation and the reduction in cold bias is improving land sea thermal contrast feeding back to the circulation and improving moisture transport. However, in 2012 and 2013 relative improvement in the cold bias is confined to some part of AS, BoB, and south Indian Ocean only, hence consequent improvement in moisture distribution is less. More importantly, the cold bias in the BoB is reduced, where most of the weather systems form during the monsoon season. Figures 8a–8c display the seasonal mean as well as month wise SST bias over the Indian Ocean from CTRL and AcSAL for the study period. The analysis reveals that seasonal mean SST bias is negative in both experiments but reduced in AcSAL experiments by 0.3–0.4°C. This indicates that SST underlying the low-level

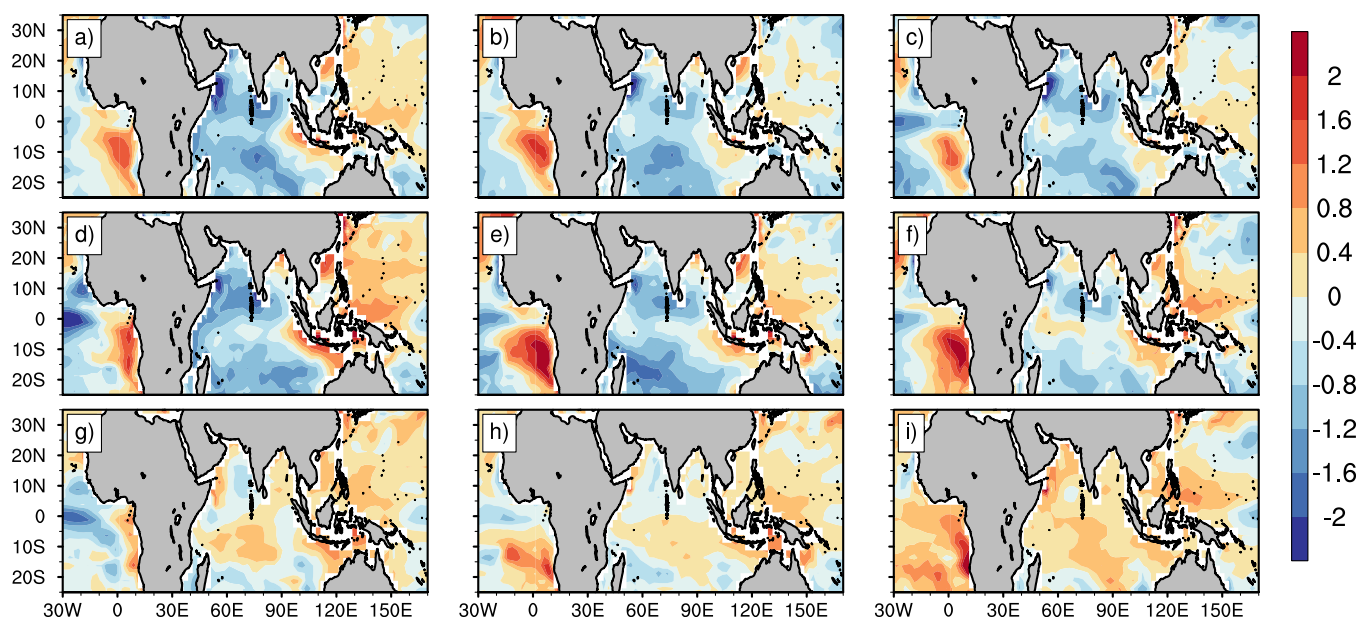


Figure 7. Spatial distribution of seasonal (JJAS) mean SST bias (°C) in (a–c) CTRL, (d–f) AcSAL with respect to HadISST, and (g–i) their difference (AcSAL-CTRL) for 2012, 2013, and 2014.

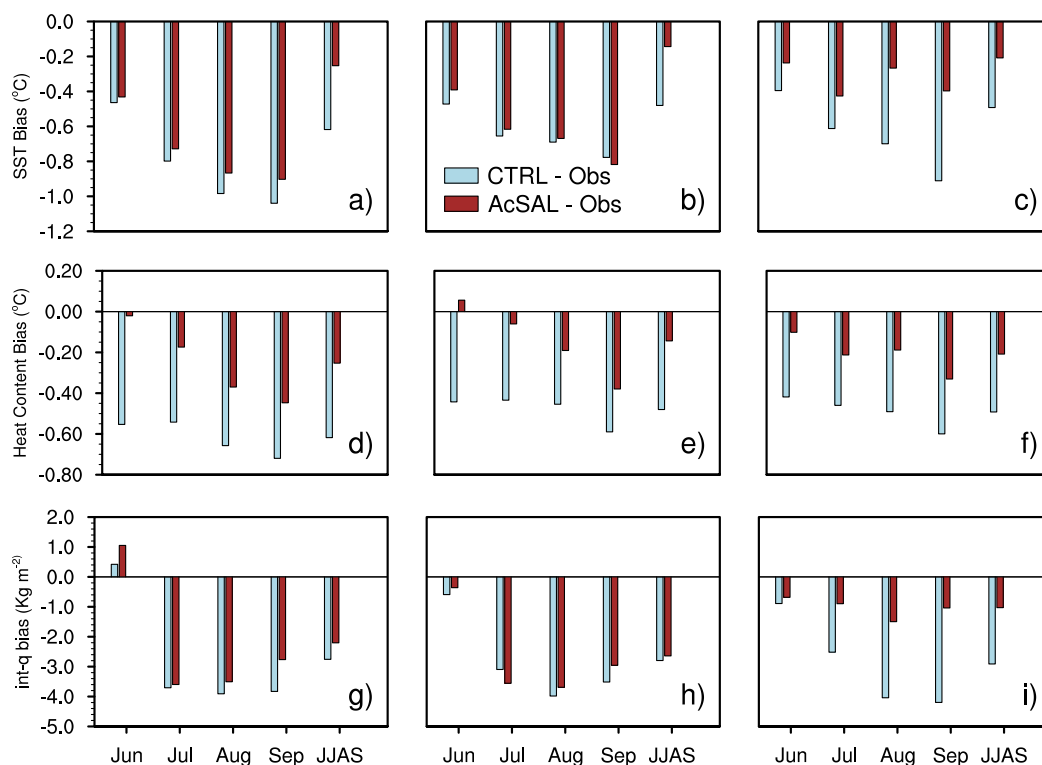


Figure 8. Monthly and seasonal mean biases of (a–c) SST, (d–f) Heat Content, and (g–i) Integrated moisture over Indian Ocean (15°S:25°N, 40:100°E) for 2012, 2013, and 2014.

monsoon circulation is more realistic in the AcSAL compared to CTRL. These results are consistent with Saha et al. (2016), which reported that improper representation of Indian Ocean SST prediction limits the predictability of ISM. Figures 8d–8f show seasonal mean as well as month wise upper ocean heat content bias over the Indian Ocean from CTRL and AcSAL for the 3 year summer monsoon. Reduction in the upper ocean heat content bias by 0.3–0.4°C is clearly evident from this analysis. These findings support that the assimilation of actual salinity profiles and high-resolution forcing lead to better upper ocean temperature state in OICs. This OICs based hindcast display improvement in the evolution of SST and heat content throughout the season. Which leads to realistic coupling processes and better air-sea interaction in the coupled model, culminating with realistic moisture transport toward the land (Figure 8g–8h). These processes enforce better tropospheric temperature and rainfall seasonal forecast in the AcSAL resulting in the diminishing of the prominent dry bias over the ISM region.

4. Summary and Conclusions

The main objective of the present study is to explore the impact of actual salinity profile data assimilation on Indian Summer Monsoon (ISM) forecast/hindcast in the coupled model CFSv2. Two hindcast experiments (CTRL and AcSAL) are carried out for the summer monsoons of 2012–2014, in which only the ocean initial conditions (OICs) differ. In CTRL OICs are generated by NCEP-GODAS, in which temperature observations from multiple sources such as XBTs, ships, satellites, Argo etc. along with synthetic salinity profiles are assimilated. Whereas, in AcSAL experiment OICs are generated by IITM-GODAS, in which only Argo observed temperature and actual salinity profiles are assimilated. IITM-GODAS is based on NCMWRF high-resolution atmospheric forcing fields. However, NCEP-GODAS is based on NCEP-R2 atmospheric forcing fields. The CFSv2 model physics, setup, and atmospheric initial conditions are same for both CTRL and AcSAL experiments. These experiments are 10 members hindcast for 3 years (2012–2014) summer monsoon, initiated from May month and hindcast for the next 9 months. Major issues in CTRL are cold SST, dry troposphere, cold tropospheric temperature, and underestimation of rainfall over the MCR with respect to observations and reanalysis products. In AcSAL, seasonal mean and monthly analysis of rainfall for the MCR

and all-India display about 10% reduction in dry bias compared to CTRL. Spatial distribution of rainfall for summer season from AcSAL indicates reduction in the prominent dry bias over Indian land region and wet bias over the oceanic region.

Detailed analysis reveals that actual salinity assimilation based OICs improved the upper ocean stability over the tropical global ocean in general and to the BoB and south eastern AS in particular. Upper ocean stability is nothing but the manifestation of vertical gradient of density (Fousiya et al., 2015, Karmakar et al., 2017), which is also presented by the Brunt-Vaisala frequency. This proper representation of upper ocean stability is mandatory for the better simulation of upper ocean mixing, however synthetic salinity profile assimilation underestimates the upper ocean stability (Huang et al., 2008) and allows excess upper ocean mixing in the model resulting cold bias to the upper ocean temperature (Chowdary et al., 2016). However, in case of actual salinity assimilation (AcSAL) better representation of stability improves representation of mixing which in turn reduces cold biases in the temperature and reduces the underestimation of upper ocean heat content throughout the season. This improvement reduces dominant cold SST bias of CFSv2 and produces better air-sea interaction, and positively feedback to improved exchange of moisture through evaporation to the atmosphere. The improvement in the SST distribution over the Indian Ocean leads to better monsoon circulation in the AcSAL than CTRL. This improves moisture transport to the Indian land mass and reduces negative bias of moisture over the AS and MCR, produces better diabatic heating and reduces tropospheric temperature bias. This improvement in tropospheric temperature better represents the meridional gradient, positively feedback to the vertical shear of horizontal winds, and supports more realistic monsoon features (Goswami et al., 2014). These all improvements in AcSAL compared to CTRL result in the reduction of dry biases throughout the season and throughout the ISM region. Thus, it is recommended that high-resolution forcing and actual salinity profile should be used to prepare the OICs for better seasonal prediction of ISM rainfall.

Acknowledgments

Authors would like to thank the Director IITM, Pune. IITM is fully funded by MoES, Government of India, New Delhi. Authors duly acknowledge National Centre for Atmospheric Research (NCAR) for making available the NCAR Command Language and National Oceanic and Atmospheric Administration (NOAA) for providing the CFSv2 initial conditions through National Operational Model Archive and Distribution System. The HYCOM analysis that we have used can be found here: <https://hycom.org/data/glbOpt08/expt-91pt1>. We sincerely thank anonymous reviewers for their valuable comments that helped us to improve the manuscript. Model data for this paper are presently available on request basis later it may be provided on open access.

References

- Adler, R. F., Huffman, G. J., Chang, A., Ferraro, R., Xie, P.-P., Janowiak, J., et al. (2003). The version-2 global rainfall climatology project (GPCP) monthly precipitation analysis (1979–present). *Journal of Hydrometeorology*, 4, 1147–1167.
- Agarwal, N., Sharma, R., Parekh, A., Basu, S., Sarkar, A., & Agarwal, V. K. (2012). Argo, Observations of barrier layer in the tropical Indian Ocean. *Advances in Space Research*, 50, 642–654. <https://doi.org/10.1016/j.asr.2012.05.021>
- Alves, O., Balmaseda, M. A., Anderson, D., & Stockdale, T. (2004). Sensitivity of dynamical seasonal predictions to ocean initial conditions. *Quarterly Journal of the Royal Meteorological Society*, 130, 647–667.
- Argo Science Team (2001). The global array of profiling floats. In C. J. Koblnsky & N. R. Smith (Eds.), *Observing the ocean in the 21st century* (pp. 248–258). Melbourne, Australia: Australian .
- Ashok, K., Zhao Yong, G., & Yamagata, T. (2001). Impact of the Indian Ocean dipole on the relationship between the Indian monsoon rainfall and ENSO. *Geophysical Research Letters*, 28(23), 4499–4502. <https://doi.org/10.1029/2001GL013294>
- Balmaseda, M. A., & Anderson, D. (2009). Impact of initialization strategies and observations on seasonal prediction skill. *Geophysical Research Letters*, 36, L01701. <https://doi.org/10.1029/2008GL035561>
- Behringer, D. W. (2007). *The Global Ocean data assimilation system at NCEP*. Paper presented at 11th Symposium on Integrated Observing and Assimilation Systems for Atmosphere, Oceans, and Land Surface, American Meteorological Society, San Antonio, Texas.
- Behringer, D. W., & Xue, Y. (2004). *Evaluation of the global ocean data assimilation system at NCEP: The Pacific Ocean*. Paper presented at Eighth symposium on Integrated Observing and Assimilation Systems for Atmosphere, Oceans, and Land Surface, AMS 84th Annual Meeting, Washington State Convention and Trade Center, Seattle, Washington.
- Bombardi, R. J., Tawfik, A. B., Manganello, J. V., Marx, L., Shin, C.-S., Halder, S., et al. (2016). The heated condensation framework as a convective trigger in the NCEP climate forecast system version 2. *Journal of Advances in Modeling Earth Systems*, 8, 1310–1329. <https://doi.org/10.1002/2016MS000668>
- Charney, J. G., & Shukla, J. (1981). Predictability of monsoons. In J. Lighthill & R. P. Pearce (Eds.), *Monsoon dynamics* (pp. 99–109). Cambridge, UK: Cambridge University Press.
- Chowdary, J. S., Parekh, A., Sayantani, O., & Gnanaseelan, C. (2015). Role of upper ocean processes in the seasonal SST evolution over tropical Indian Ocean in climate forecasting system. *Climate Dynamics*, 45, 2387–2405. <https://doi.org/10.1007/s00382-015-2478-4>
- Chowdary, J. S., Parekh, A., Srinivas, G., Gnanaseelan, C., Fousiya, T. S., Khandekar, R., et al. (2016). Processes associated with the tropical Indian Ocean subsurface temperature bias in a coupled model. *Journal of Physical Oceanography*, 46, 2863–2875. <https://doi.org/10.1175/JPO-D-15-0245.1>
- Cummings, J. A. (2005). Operational multivariate ocean data assimilation. *Quarterly Journal of the Royal Meteorological Society*, 131, 3583–3604.
- Cummings, J. A., & Smedstad, O. M. (2013). Variational data assimilation for the global ocean. In S. K. Park & L. Xu (Eds.), *Data assimilation for atmospheric, oceanic and hydrologic applications* (Vol. II, pp. 303–343). Berlin, Germany: Springer.
- De, S., Hazra, A., & Chaudhari, H. S. (2016). Does the modification in “critical relative humidity” of NCEP CFSv2 dictate Indian mean summer monsoon prediction? Evaluation through thermodynamical and dynamical aspects. *Climate Dynamics*, 46, 1197–1222. <https://doi.org/10.1007/s00382-015-2640-z>
- Dee, D. P., Uppala, S. M., Simmons, A. J., Berrisford, P., Poli, P., Kobayashi, S., et al. (2011). The ERA-interim reanalysis: Configuration and performance of the data assimilation system. *Quarterly Journal of the Royal Meteorological Society*, 137, 553–597. <https://doi.org/10.1002/qj.828>
- Deshpande, A., Gnanaseelan, C., Chowdary, J. S., Rahul, S. (2017). Interannual spring Wyrтки jet variability and its regional impacts. *Dynamics of Atmosphere and Ocean*, 78, 26–37. <https://doi.org/10.1016/j.jydmatmoe.2017.02.001>

- Fischer, M., Latif, M., Flugel, M., & Ji, M. (1997). The impact of data assimilation on ENSO simulations and predictions. *Monthly Weather Review*, *125*, 819–830.
- Fousiya, T. S., Parekh, A., & Gnanaseelan, C. (2015). Interannual variability of upper ocean stratification in Bay of Bengal: Observational and modeling aspects. *Theoretical and Applied Climatology*, *126*, 285–301. <https://doi.org/10.1007/s00704-015-1574-z>
- Ganai, M., Mukhopadhyay, P., Krishna, R. P. M., & Mahakur, M. (2015). The impact of revised simplified Arakawa-Schubert convection parameterization scheme in CFSv2 on the simulation of the Indian summer monsoon. *Climate Dynamics*, *45*, 881–902. <https://doi.org/10.1007/s00382-014-2320-4>
- Goswami, B. B., Deshpande, M., Mukhopadhyay, P., Saha, S. K., Rao, S. A., Murthugudde, R., et al. (2014). Simulation of monsoon intraseasonal variability in NCEP CFSv2 and its role on systematic bias. *Climate Dynamics*, *43*, 2725–2745. <https://doi.org/10.1007/s00382-014-2089-5>
- Goswami, B. N., Ajayamohan, R. S., Xavier, P. K., & Sengupta, D. (2003). Clustering of synoptic activity by Indian summer monsoon intraseasonal oscillations. *Geophysical Research Letters*, *30*(8), 1431. <https://doi.org/10.1029/2002GL016734>
- Goswami, B. N., & Xavier, P. K. (2005). ENSO control on the south Asian monsoon through the length of the rainy season. *Geophysical Research Letters*, *32*, L18717. <https://doi.org/10.1029/2005GL023216>
- Goswami, T., Rao, S. A., Hazra, A., Chaudhari, H. S., Dhakate, A., Salunke, K., et al. (2017). Assessment of simulation of radiation in NCEP Climate Forecasting System (CFS V2). *Atmospheric Research*, *193*, 94–106. <https://doi.org/10.1016/j.atmosres.2017.04.013>
- Good, S. A., Martin, M. J., & Rayner, N. A. (2013). EN4: Quality controlled ocean temperature and salinity profiles and monthly objective analyses with uncertainty estimates. *Journal of Geophysical Research: Oceans*, *118*, 6704–6716. <https://doi.org/10.1002/2013JC009067>
- Griffies, S. M., Harrison, M. J., Pacanowski, R. C., & Rosati, A. (2004). *A technical guide to MOM4* (GFDL Ocean Group Tech. Rep. 5:371). Princeton, NJ: NOAA/Geophysical Fluid Dynamics Laboratory.
- Hazra, A., Chaudhari, H. S., Rao, S. A., Goswami, B. N., Dhakate, A., Pokhrel, S., et al. (2015). Impact of revised cloud microphysical scheme in CFSv2 on the simulation of the Indian summer monsoon. *International Journal of Climatology*, *35*, 4738–4755.
- Huang, B., Xue, Y., & Behringer, D. W. (2008). Impacts of Argo salinity in NCEP global ocean data assimilation system: The tropical Indian Ocean. *Journal of Geophysical Research*, *113*, C08002. <https://doi.org/10.1029/2007JC004388>
- Ji, M., & Leetmaa, A. (1997). Impact of data assimilation on ocean initialization and El Niño prediction. *Monthly Weather Review*, *125*, 742–753.
- Kakatkar, R., Gnanaseelan, C., Chowdary, J. S., Parekh, A., & Deepa, J. S. (2017). Indian summer monsoon rainfall variability during 2014 and 2015 and associated Indo-Pacific upper ocean temperature patterns. *Theoretical and Applied Climatology*, *131*, 1235–1247. <https://doi.org/10.1007/s00704-017-2046-4>
- Kalnay, E. (2002). *Atmospheric modeling, data assimilation, and predictability* (341 p.). Cambridge, UK: Cambridge University Press.
- Kanamitsu, M., Ebisuzaki, W., Woollen, J., Yang, S. K., Hnilo, J. J., Fiorino, M., et al. (2002). NCEP-DOE AMIP-II reanalysis (R-2). *Bulletin of the American Meteorological Society*, *83*, 1631–1643.
- Karmakar, A., Parekh, A., Chowdary, J. S., & Gnanaseelan, C. (2017). Inter comparison of Tropical Indian Ocean features in different ocean reanalysis products. *Climate Dynamics*, *8*, 1–23. <https://doi.org/10.1007/s00382-017-3910>
- Kim, H. M., Webster, P. J., Curry, J. A., & Toma, V. E. (2012). Asian summer monsoon prediction in ECMWF system 4 and NCEP CFSv2 retrospective seasonal predictions. *Climate Dynamics*, *39*(12), 2975–2991.
- Kumar, K., Hoerling, M., & Rajagopalan, B. (2005). Advancing dynamical prediction of Indian monsoon rainfall. *Geophysical Research Letters*, *32*, L08704. <https://doi.org/10.1029/2004GL021979>
- Kumar, K., Soman, M. K., & Rupa Kumar, K. (1995). Seasonal prediction of Indian summer monsoon rainfall: A review. *Weather*, *50*, 449–467.
- Levine, R. C., & Turner, A. G. (2012). Dependence of Indian monsoon rainfall on moisture fluxes across the Arabian Sea and the impact of coupled model sea surface temperature biases. *Climate Dynamics*, *38*, 2167–2190.
- Mooley, D. A., & Shukla, J. (1989). Main features of the westward-moving low pressure systems which form over the Indian region during the summer monsoon season and their relation to the monsoon rainfall. *Mausam*, *40*, 137–152.
- Narapusetty, B., Murtugudde, R., Wang, H., & Kumar, A. (2015). Ocean-atmosphere processes driving Indian summer monsoon biases in CFSv2 hindcasts. *Climate Dynamics*, *47*, 1417–1433. <https://doi.org/10.1007/s00382-015-2910-9>
- Pai, D. S., Sridhar, L., Badwaik, M. R., & Rajeevan, M. (2014). Analysis of the daily rainfall events over India using a new long period (1901–2010) high resolution (0.25° × 0.25°) gridded rainfall data set. *Climate Dynamics*, *45*, 755–776. <https://doi.org/10.1007/s00382-014-2307-1>
- Palmer, T. N., & Anderson, D. L. T. (1994). The prospects for seasonal prediction. *Quarterly Journal of the Royal Meteorological Society*, *120*, 755–793.
- Pant, G. B., & Parthasarathy, B. (1981). Some aspects of an association between the Southern Oscillation and Indian summer monsoon. *Archives for Meteorology, Geophysics, and Bioclimatology, Series B*, *29*, 245–251.
- Parekh, A., J. S., Chowdary, O. S., T. S., Fousiya, C., & Gnanaseelan, (2016). Tropical Indian Ocean surface salinity bias in climate prediction system coupled models and the role of upper ocean processes. *Climate Dynamics*, *46*, 2403–2422.
- Parthasarathy, B., Munot, A. A., & Kothawale, D. R. (1995). All India monthly and seasonal rainfall series: 1871–1993. *Theoretical and Applied Climatology*, *49*, 217–224.
- Pathak, A., Ghosh, S., Kumar, P., & Murtugudde, R. (2017). Role of oceanic and terrestrial atmospheric moisture sources in intraseasonal variability of Indian, Summer Monsoon rainfall. *Scientific Reports*, *7*, 12729. <https://doi.org/10.1038/s41598-017-13115-7>
- Pisharoty, P. R. (1965). Evaporation from the Arabian Sea and the Indian Southwest Monsoon. In *Proceedings of International Indian Ocean Expedition* (pp. 43–54). Mumbai, India: IIOE.
- Pokhrel, S., Rahaman, H., Parekh, A., Saha, S. K., Dhakate, A., Chaudhari, H. S., et al. (2012). Evaporation-rainfall variability over Indian Ocean and its assessment in NCEP climate prediction system (CFSv2). *Climate Dynamics*, *39*, 2585–2608.
- Pokhrel, S., Saha, S. K., Dhakate, A., Rahman, H., Chaudhari, H. S., Salunke, K., et al. (2016). Seasonal prediction of Indian summer monsoon rainfall in NCEP CFSv2: prediction and predictability error. *Climate Dynamics*, *1*, 2305–2326. <https://doi.org/10.1007/s00382-015-2703>
- Rahaman, H., Behringer, D. W., Penny, S. G., & Ravichandran, M. (2016). Impact of an upgraded model in the NCEP global ocean data assimilation system: The tropical Indian Ocean. *Journal of Geophysical Research: Oceans*, *121*, 8039–8062. <https://doi.org/10.1002/2016JC012056>
- Rajagopal, E. N., Iyengar, G. R., George, J. P., Das Gupta, M., Mohandas, S., Siddharth, R., et al. (2012). *Implementation of unified model based analysis-forecast system at NCMRWF* (Tech. Rep. NCMRF/TR/2/2012, NCMRWF). New Delhi, India: National Centre for Medium Range Weather Forecasting, Ministry of Earth Sciences, Government of India.
- Rajeevan, M., Gadgil, S., & Bhate, J. (2010). Active and break spells of the Indian summer monsoon. *Journal of Earth System Science*, *119*(3), 229–247.
- Ramu, D. A., Sabeerali, C. T., Chattopadhyay, R., Rao, D. N., George, G., Dhakate, A. R., et al. (2016). Indian summer monsoon rainfall simulation and prediction skill in the CFSv2 coupled model: Impact of atmospheric horizontal resolution. *Journal of Geophysical Research: Atmospheres*, *121*, 2205–2221. <https://doi.org/10.1002/2015JD024629>

- Rasmusson, E. M., & Carpenter, T. H. (1983). The relationship between eastern equatorial Pacific sea surface temperature and rainfall over India and Sri Lanka. *Monthly Weather Review*, *111*, 517–528.
- Rayner, N. A., Parker, D. E., Horton, E. B., Folland, C. K., Alexander, L. V., Rowell, D. P., et al. (2003). Global analyses of sea surface temperature, sea ice, and night marine air temperature since the late nineteenth century. *Journal of Geophysical Research*, *108*(D14), 4407. <https://doi.org/10.1029/2002JD002670>
- Saha, K. R., & Bavadekar, S. N. (1973). Water vapour budget and rainfall over the Arabian Sea during the northern summer. *Quarterly Journal of the Royal Meteorological Society*, *99*, 273–278.
- Saha, S., Moorthi, S., Pan, H.-L., Wu, X., Wang, J., Nadiga, S., et al. (2010). The NCEP climate prediction system reanalysis. *Bulletin of the American Meteorological Society*, *91*(8), 1015–1057.
- Saha, S., Moorthi, S., Wu, X., Wang, J., Nadiga, S., Tripp, P., et al. (2014). The NCEP climate prediction system version 2. *Journal of Climate*, *27*, 2185–2208.
- Saha, S. K., Pokhrel, S., Kiran, S., Dhakate, A., Chaudhari, H. S., Rahaman, H., et al. (2016). Potential predictability of Indian summer monsoon rainfall in NCEP CFSv2. *Journal of Advances in Modeling Earth Systems*, *8*, 96–120. <https://doi.org/10.1002/2015MS000542>
- Shenoi, S. S. C., Shankar, D., & Shetye, S. R. (2002). Differences in heat budgets of the near-surface Arabian Sea and Bay of Bengal: Implications for the summer monsoon. *Journal of Geophysical Research*, *107*(C6), 3052. <https://doi.org/10.1029/2000JC000679>
- Sikka, D. R. (1980). Some aspects of the large-scale fluctuations of summer monsoon rainfall over India in relation to fluctuations in the planetary and regional scale circulation parameters. *Proceedings of the Indian Academy of Sciences: Earth and Planetary Sciences*, *89*, 179–195.
- Sreenivas, P., Gnanaseelan, C., Kakatkar, R., Pavan Kumar, N., Chowdary, J. S., Parekh, A., et al. (2015). *Implementation and validation of global ocean data assimilation system at IITM* (IITM Sci. (Research) Rep. ESSO/IITM/SERP/SR/01(2015)/184). Pune, India: Indian Institute of Tropical Meteorology, Earth System Science Organization, Ministry of Earth Sciences.
- Srinivas, G., Chowdary, J. S., Gnanaseelan, C., Prasad, K. V. S. R., Karmakar, A., et al. (2017). Association between mean and interannual equatorial Indian Ocean subsurface temperature bias in a coupled model. *Climate Dynamics*, 1–15. <https://doi.org/10.1007/s00382-017-3713-y>
- Thompson, B., Gnanaseelan, C., & Salvekar, P. S. (2006). Seasonal evolution of temperature inversions in the north Indian Ocean. *Current Science*, *90*(5), 697–704.
- Vörösmarty, C. J., Willmott, C. J., Choudhury, B. J., Schloss, A. L., Stearns, T. K., Robeson, S. M., et al. (1996). Analyzing the discharge regime of a large tropical river through remote sensing, ground-based climatic data, and modeling. *Water Resources Research*, *32*(10), 3137–3150. <https://doi.org/10.1029/96WR01333>
- Webster, P. J., & Yang, S. (1992). Monsoon and ENSO: Selectively interactive systems. *Quarterly Journal of the Royal Meteorological Society*, *118*, 877–926.
- Xavier, P. K., Marzin, C., & Goswami, B. N. (2007). An objective definition of the Indian summer monsoon season and a new perspective on the ENSO-monsoon relationship. *Quarterly Journal of the Royal Meteorological Society*, *133*, 749–764.
- Yang, S. C., Rienecker, M., & Keppenne, C. (2010). The impact of ocean data assimilation on seasonal-to-interannual predictions: A case study of the 2006 El Niño event. *Journal of Climate*, *23*, 4080–4095.
- Yu, L., & Weller, R. A. (2007). Objectively analyzed air-sea heat fluxes for the global ice-free oceans (1981–2005). *Bulletin of the American Meteorological Society*, *88*, 527–539.
- Zhao, M., Hendon, H., Alves, O., & Yin, Y. (2014). Impact of improved assimilation of temperature and salinity for coupled model seasonal predictions. *Climate Dynamics*, *42*, 2565–2583.
- Zhao, M., Hendon, H., Alves, O., Yin, Y., & Anderson, D. (2013). Impact of salinity constraints on the simulated mean state and variability in a coupled seasonal prediction model. *Monthly Weather Review*, *141*, 388–402.
- Zhu, J., & Shukla, J. (2013). The role of air-sea coupling in seasonal prediction of Asia-Pacific summer monsoon rainfall. *Journal of Climate*, *26*, 5689–5697. <https://doi.org/10.1175/JCLI-D-13-00190.1>